Light scattering in translucent layers: angular distribution and internal reflections at flat interfaces

Arthur Gautheron, Raphaël Clerc, Vincent Duveiller, Lionel Simonot, Bruno Montcel, Mathieu Hebert

▶ **To cite this version:**

Arthur Gautheron, Raphaël Clerc, Vincent Duveiller, Lionel Simonot, Bruno Montcel, et al.. Light scattering in translucent layers: angular distribution and internal reflections at flat interfaces. 34 (15), pp.221-1-221-6, 2022, 10.2352/EI.2022.34.15.COLOR-221 . hal-03533893

HAL Id: hal-03533893
https://hal.science/hal-03533893v1

Submitted on 19 Jan 2022

HAL is a multi-disciplinary open access archive for the deposit and dissemination of scientific research documents, whether they are published or not. The documents may come from teaching and research institutions in France or abroad, or from public or private research centers.

L'archive ouverte pluridisciplinaire **HAL**, est destinée au dépôt et à la diffusion de documents scientifiques de niveau recherche, publiés ou non, émanant des établissements d'enseignement et de recherche français ou étrangers, des laboratoires publics ou privés.

Light scattering in translucent layers: angular distribution and internal reflections at flat interfaces

Arthur GAUTHERON [1,], Raphaël CLERC [2], Vincent DUVEILLER [2], Lionel SIMONOT [3], Bruno MONTCEL [1], Mathieu HEBERT [2]*

[1]Univ Lyon, INSA-Lyon, Université Claude Bernard Lyon 1, CNRS, Inserm, CREATIS UMR 5220, U1294, F-69621, LYON, France; [2]Univ Lyon, UJM-Saint-Etienne, CNRS, Institut d Optique Graduate School, Lab. Hubert Curien UMR 5516, F-42023, St Etienne, France ; [3]Université de Poitiers, Institut Pprime CNRS, Chasseneuil Futuroscope, France
** gautheron@creatis.insa-lyon.fr*

Abstract

Optical characterization and appearance prediction of translucent materials is needed in several fields of engineering such as computer graphics, dental restorations or 3D printing technologies. In the case of strongly diffusing materials, flux transfer models like the Kubelka-Munk model (2-flux) or 4-flux model have been successfully used to this aim for decades. However, they lead to inaccurate prediction of the color variations of translucent objects of different thicknesses. Indeed, as they assume Lambertian fluxes at any depth within the material and in particular at the bordering interfaces, they fail to model the internal reflectance at the interfaces, penalizing the accuracy of the optical parameter extraction. The aim of the paper is to investigate the impact of translucency on light angular distribution and corresponding internal reflectances, by the mean of the radiative transfer equation, which describes more rigorously the impact of the scattering on the light propagation. It turns out that the light angular distribution at the bordering interfaces, assumed to be flat, is far from being Lambertian, and the internal reflectance may vary a lot according to the layer's thickness, refractive index, scattering and absorption coefficients. This work not only enables to better understand the impact of scattering within a translucent layer but also invites to revisit the well-known Saunderson correction used in 2- or 4- flux models.

Introduction

Many fabrication processes rely on the use of translucent materials, i.e., materials in which light can enter deeply and be scattered progressively along its path. This is the case for example with some polymer inks in 3D printing, dental repair materials [1], [2], human tissues, some ceramics, and many other materials for which color management is essential. The issue with these translucent materials is that the color and general appearance depend a lot on the object's thickness, in a way that a simple light scattering model – the Kubelka-Munk (2-flux) model [3], or even the 4-flux model [4] – cannot predict accurately. One reason for the lack of accuracy of 2-flux models with translucent layers is the poor estimation of the internal reflectance of the interfaces bordering the material layer. Indeed, the Saunderson correction [5, 6] assumes usually an inaccurate Lambertian distribution of the light striking the interfaces. More importantly, the exact angular distribution depends on the scattering and absorption properties of the layer and on its thickness. Moreover, with the reflectance or transmittance measurement geometries recommended by the CIE, e.g. the d:8° or 8°:d geometries, the incident light or the captured light is directional, whereas the two-flux models expects measurements based on a bi-hemispherical geometry. This has almost no impact in strongly scattering layers but may have a significant impact in a translucent material. As an example, it has been shown recently that in dental repair material, using an internal reflectance value of 4% (instead of the expected Lambertian value of 60% for a refractive index 1.5) improves a lot the color prediction accuracy for slabs of various thicknesses [7]. In principle, these issues could be addressed using more sophisticated solutions of the Radiative Transfer Equation [8] either by direct solving or by Monte Carlo methods. However, compared to the 2- or 4-flux methods, these approaches are much more time consuming, making difficult the extraction of optical parameters from a large set of experiments.

The aim of the study is to investigate this point in detail using the formalism of the radiative transfer equation, and to compute more accurate values of the internal reflectance to be used in the simplified 2-flux model (such as the Saunderson correction for the Kubelka-Munk model [5, 6]), in function of thickness, refractive index, absorption and scattering coefficients. We first present briefly the method used to solve the radiative transfer equation in the case of homogeneous and flat scattering layers, then use it to simulate the angular radiance distribution near their interfaces, and analyze the influence of various parameters: absorption coefficient, layer thickness.

Solving the radiative transfer equation with bordering interfaces

The radiative transfer equation (RTE) was solved using the discrete ordinate method [8] [9], for a homogenous layer of thickness d in the plane parallel geometry (sometimes called "slab") for given absorption μ_a and scattering μ_s coefficients (see Fig. 1). From these coefficients, two derivate parameters are defined: the albedo $\omega_0 = \mu_s / (\mu_a + \mu_s)$, and the optical thickness $\tau_d = (\mu_a + \mu_s) d$, where d is the thickness of a layer, in m. The incident light is assumed to be a directional flux at normal incidence on the whole surface, featuring an azimuthal symmetry. In consequence, in this 1D geometry, physical quantities only depend on the depth z and zenithal angle θ. The angles $|\theta| \leq 90°$ correspond to the lower hemisphere Ω' where radiance values depict the angular distribution of the light going upwards. The other angles correspond to the upper hemisphere Ω, where radiance values depict the angular distribution of the light going towards negative values of z (therefore downwards). Boundary conditions at the interface account for the Fresnel reflection, following the methods proposed in Refs. [9] and [10]. Note that multiple reflections of the specular light are included in the source term of the RTE for diffused light, following the approach proposed in [10].

The direct solving method enables to obtain the angular radiance distribution at any depth in the layer, therefore at the two depths of interest here $z = 0$ and $z = d$. These angular distributions, resulting from the solving of the radiative transfer equation with the Fresnel angular reflectance of the interfaces, are integrated over the hemisphere to provide the expected internal reflectance.

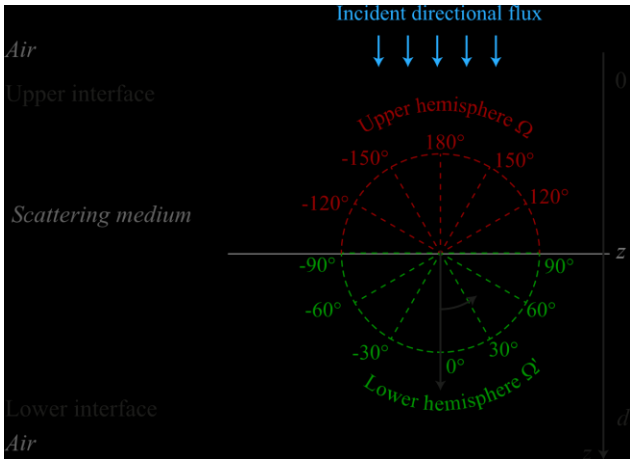

Fig. 1: Studied configuration where a layer of scattering medium with different refractive index as the surrounding air ("slab") is illuminated by directional light at normal incidence. Physical quantities depend on depth z and angle θ.

In order to validate the implemented model, benchmarks with a widely used Monte Carlo code [11] with different sets of parameters (refractive index, absorption and scattering coefficients, layer thickness, and Henyey-Greenstein phase function) were performed, considering the same geometrical configurations and physical parameters.

Semi-infinite layer

We first consider the case of a semi-infinite scattering medium (optical thickness $(\mu_a+\mu_s)d >> 1$). To simplify the discussion, the phase function was assumed to be isotropic, i.e., $g = 0$.

The main mechanisms occurring during light transport in the diffusing material are well-known and illustrated on Fig. 2. First, the incident directional flux can be either reflected by the top interface or transmitted in the medium, where it is progressively scattered or absorbed. Some light propagating upwards may reach the interface, where it can be either transmitted or reflected. Note that all light rays with incident angle higher than the critical angle $i_c = \arcsin(1/n)$ are necessarily reflected (total internal reflection). It must be noted that in the semi-infinite material, the light that propagates upwards has necessarily undergone one or several scattering events.

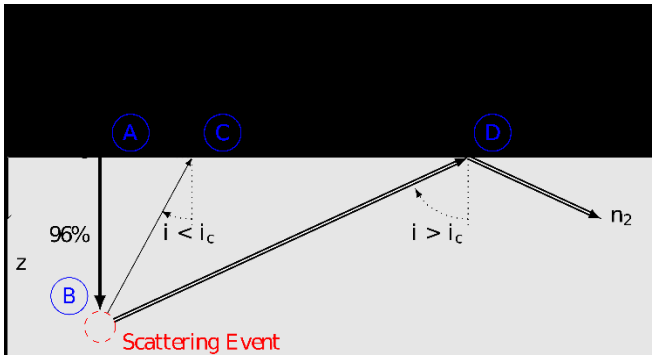

Fig. 2: Photon trajectory inside a semi-infinite layer of scattering medium (refractive index $n_2 = n$) under collimated incident light (flux F_0). The incident light can be either reflected at the interface (A) or transmitted into the medium. After a scattering event (B), a photon may propagate until reaching the interface. If the incident angle is below the critical angle i_c, it can exit the medium or be reflected (C). If it is higher than i_c, it is totally reflected back to the medium (D). Percentages are given for n=1.5.

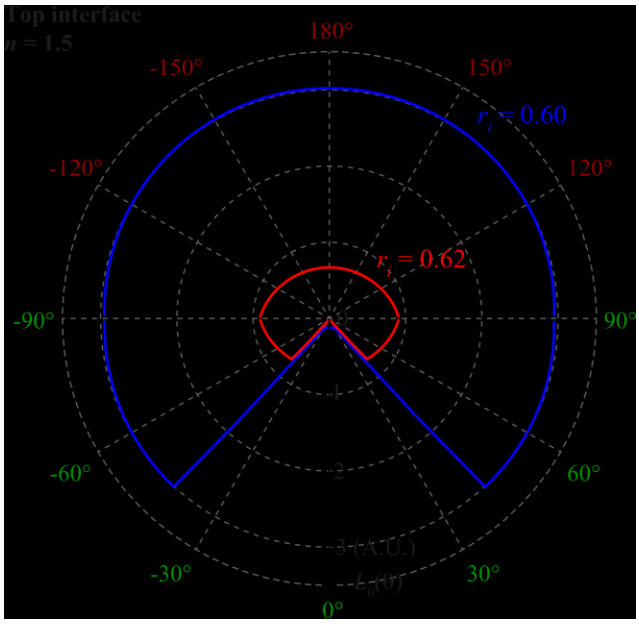

Fig. 3: Cut view of the relative angular radiance diagram near the top interface for semi-infinite scattering layers of two media of refractive index n = 1.5, with g = 0: a non-absorbing medium of scattering coefficient μ_s =5.0 mm^{-1} and albedo ω0 = 1 (blue curve), and an absorbing medium of extinction coefficient $(\mu_a+\mu_s)$ = 5.0 mm^{-1} and albedo ω0 = μ_s / $(\mu_a+\mu_s)$ = 0.9 (red curve). The light illuminating the interface from inside the layer propagates with zenithal angles |θ| > 90° whereas the reflected light propagates with angles |θ| < 90°.

Let's us now discuss the collective impact of these mechanisms on the overall radiance angular distribution at the top interface. In Fig. 3 are plotted, in polar coordinates, cut-views of the relative angular radiance $L_z(\theta)$ at $z = 0$, or $L_0(\theta)$, as a function of the angle θ defined in Fig. 1, for a non-absorbing medium (blue curve) or absorbing medium (red curve).

In the case of a non-absorbing semi-infinite material (blue curve), the light that propagates upwards, after backscattering, is Lambertian: the radiance is a constant L_u, the graph draws a hemi-circle. This is expected, and in agreement with common assumptions made in the literature. In the lower hemisphere, as set by the boundary conditions, the downward radiance $L_0(\theta)$ is the result of the internal reflection of the radiance propagating upwards, therefore the product of radiance L_u with the Fresnel reflectance. For a refractive index n of 1.5, this later is equal to 0.04 at $\theta = 0°$, and suddenly reaches 1 beyond the critical angle $i_c = \arcsin(1/n) \approx 42°$. Let's examine the corresponding internal reflection coefficient r_i. The later is defined as :

$$r_i = \frac{\int_{0°}^{90°} L_0(180°-\theta) R_f(\theta) \sin(2\theta) d\theta}{\int_{0°}^{90°} L_0(180°-\theta) \sin(2\theta) d\theta} \qquad (1)$$

where $R_f(\theta)$ is the Fresnel angular reflectance of the material-air interface when light comes at an angle θ from the medium (therefore when the angle is 180° – θ in our radiance diagram, where the light striking the interface propagates with zenithal angles $|\theta| > 90°$). As the upward light is Lambertian (the radiance $L_0(\theta)$ is constant over the hemisphere Ω), we have $r_i = 0.60$.

In the case of an absorbing semi-infinite medium (red curve), the overall radiance is lower than in the non-absorbing case, as expected. Moreover, we observe that the upward radiance (in the

upper hemisphere) is not constant any more: it is higher as the angle θ increases. The light propagating upwards is therefore not Lambertian. Let us comment this discrepancy. First, remind that at $z = 0$, the upward radiance results from the backscattering of specular light and diffuse light propagating downwards. As previously seen, the latter is not Lambertian, because of the angular dependency of the Fresnel reflection. However, in the non-absorbing case, the upward radiance results from an infinite number of isotropic scattering events, whereas in the absorbing case, from only a limited number of scattering events. In consequence, although isotropic, scattering fails to perfectly randomize the light direction, which explains why the contribution of lower angles is lower than the contribution of higher angles to the upward radiance. The anisotropy of $L_0(\theta)$ modifies the calculation of the internal reflectance r_i. In this case, the numerator of Eq. (1) does not change much whereas the denominator decreases, resulting in an increase of r_i (see Fig. 6).

Layer with finite thickness

We now consider the case of a layer of finite thickness. Total internal reflection may occur at both interfaces in a similar way, although the situation of each interface is not symmetrical, as the specular light enters from the top interface only. In this case, not only the top (denoted r_i) but also the bottom (denoted r_i') internal reflectance require attention.

Fig. 4 (resp. Fig. 5) represents the radiances $L_0(\theta)$ and $L_d(\theta)$ at the top and bottom interfaces as functions of the zenithal angle in absence of absorption (respectively in presence of absorption), for various optical thicknesses of the medium (the sum of the absorption and scattering coefficients remaining constant in our simulations).

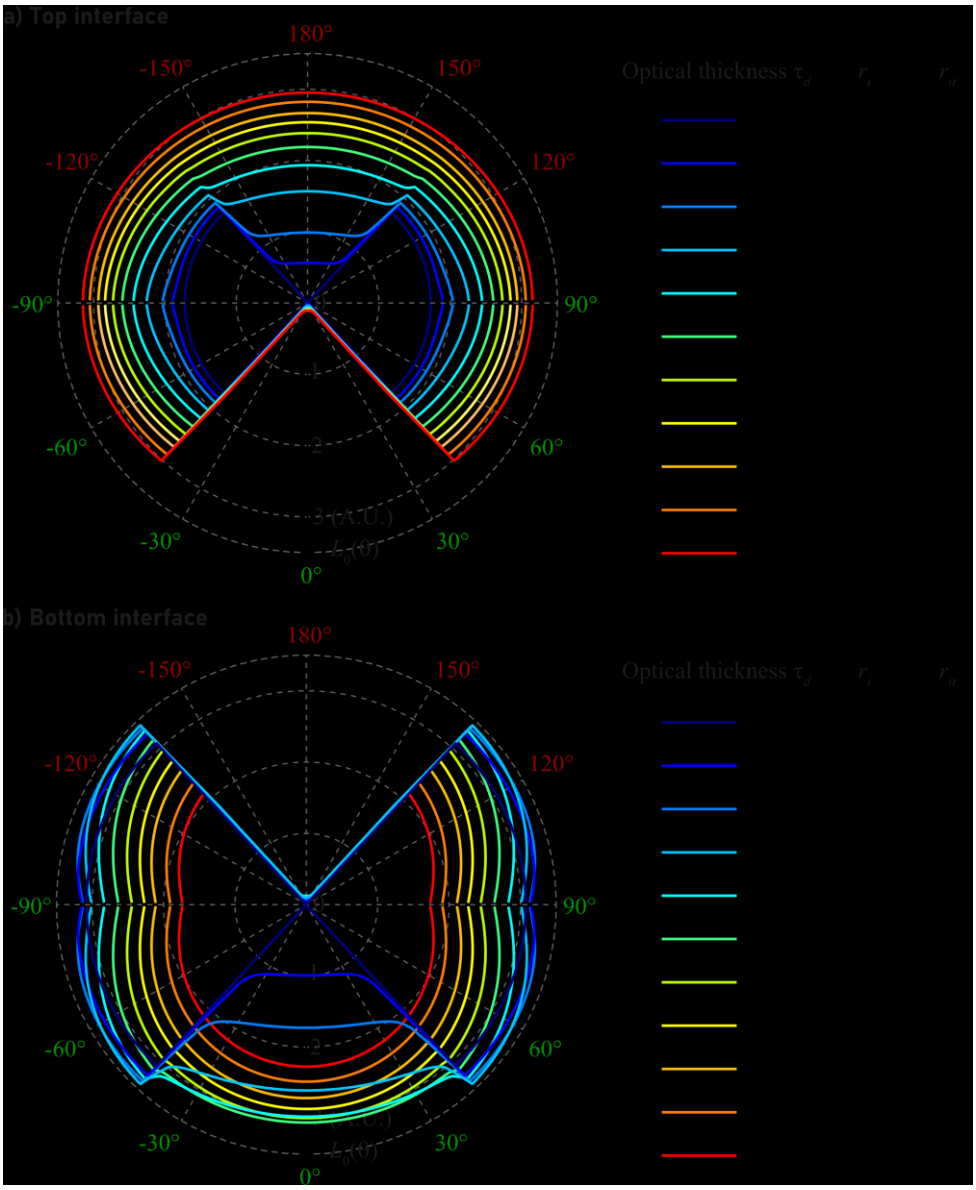

Fig. 4: Polar plot of the radiance at the top interface, $L_0(\theta)$ (Fig. 4a), and the bottom interface, $L_d(\theta)$ (Fig. 4b), for layers of different optical thicknesses in absence of absorption (refractive index n = 1.5, albedo $\omega 0 = \mu_s / (\mu_a+\mu_s)=1.0$).

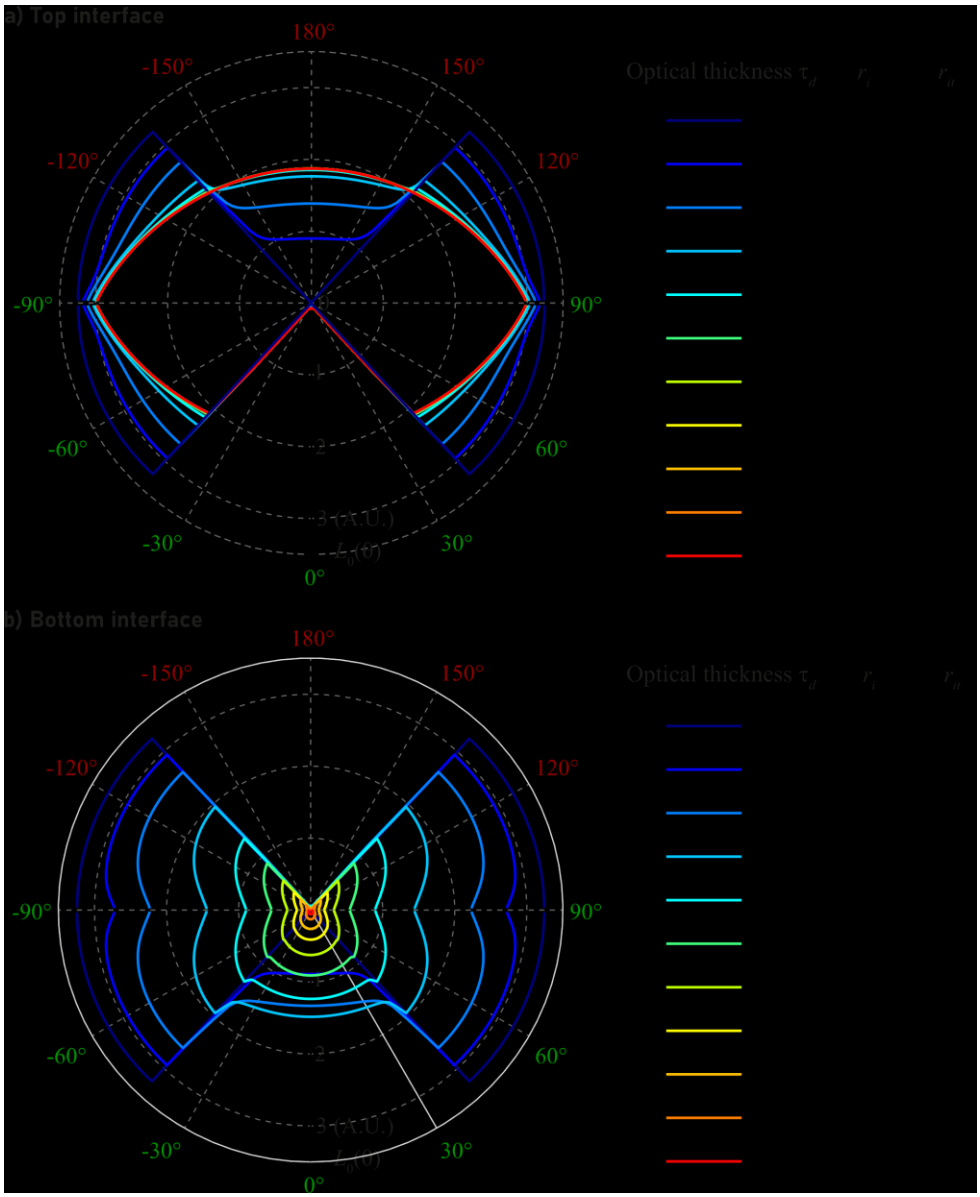

Fig. 5: Polar plot of the radiance at the top $L_0(\theta)$ (Fig. 5a) and bottom $L_d(\theta)$ (Fig. 5b) for layers of different optical thicknesses in presence of absorption (refractive index n = 1.5, albedo ω0 = μs / (μa+μs)=0.7).

With or without absorption, for a large optical thickness, i.e., $(\mu_a + \mu_s)\, d \gg 1$ (red-orange curves), the radiance distribution at the top interface tends to the one observed for a semi-infinite medium discussed in the previous section (Fig. 3): the slab behaves as a semi-infinite medium. In absence of absorption, the radiance distribution at the bottom interface also tends to be a constant, and thus, $r_i = r_i'$. In presence of absorption, the radiance distribution at the bottom interface tends to be negligible for large optical thicknesses. Even if it is possible (although difficult) to compute an internal reflectance at this bottom interface, this quantity no longer has a physical meaning nor any interest with these very small radiance values.

When $(\mu_a + \mu_s)d \ll 1$ (blue curves), however, the impact of scattering becomes negligible. We thus observed the same trend at both interfaces, in presence or in absence of absorption: radiances $L_0(\theta)$ and $L_d(\theta)$ become almost negligible for incidence angles lower than the critical angle i_c. Indeed, lower incidence angles are extracted at each interface and are no longer compensated by scattering. In consequence, upward and downward radiance become almost identical at each interface. For this reason, the numerator and denominator of equation (1) tends to be equal for each internal reflectance, resulting in an internal reflectance close to one when d tends to zero.

Notice that the same results are obtained when the absorption and scattering coefficients are multiplied by a certain factor and the layer thickness is divided by the same factor: the optical thickness, which is the relevant parameter in the model, remains constant in this case.

The internal reflectances of the top and bottom interfaces, respectively r_i and r_i', are plotted in Fig. 6, resp. Fig. 7, as

functions of the optical thickness for various albedo values. We retrieve the fact that when d, thereby the optical thickness τ_d, is very small, the internal reflectance value tends to 1 at both interfaces. As the optical thickness increases, the internal reflectance decreases. It asymptotically approaches 0.60, the value usually considered in the Saunderson model, for the top interface when the medium is strongly absorbing (low ω_0 values), or a higher value than 0.6 if the medium is less absorbing (0.63 when $\omega_0 = 1$, i.e., the medium is non-absorbing, as featured also in Fig. 4). At the bottom interface, beyond an optical thickness around 2, the internal reflectance value is below 0.60.

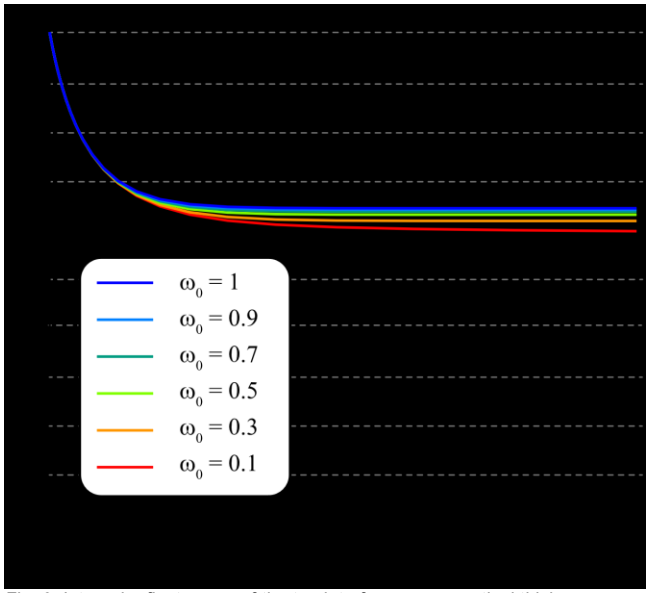

Fig. 6: Internal reflectance r_i of the top interface versus optical thickness $(\mu_a+\mu_s)$ d for several albedo $\omega_0 = \mu_s / (\mu_a+\mu_s)$ with $\mu_a+\mu_s = 5\ cm^{-1}$. The bold dashed line at $r_i = 0.6$ corresponds to the value usually considered in the classical Sanderson.

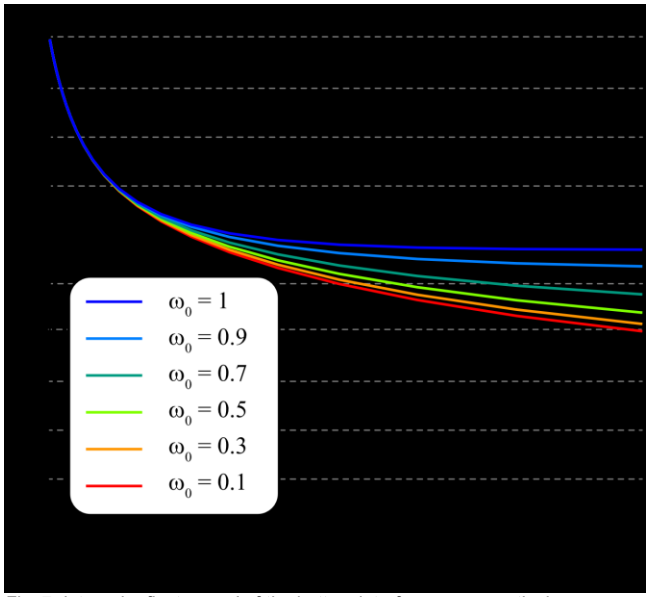

Fig. 7: Internal reflectance r_i' of the bottom interface versus optical thickness $(\mu a+\mu s)$ d for various albedo values $\omega_0 = \mu s / (\mu_a+\mu_s)$ with $\mu_a+\mu_s = 5\ cm^{-1}$. The bold dashed line at $r_i' = 0.6$ corresponds to the value usually considered in the classical Sanderson.

Conclusions

Detailed simulations based on the numerical solution of the radiative transfer equation were used to calculate the internal diffuse reflectance, a parameter needed in the efficient 2-flux or 4-flux models used for optical parameter extraction and appearance prediction. In this work, only isotropic scattering was considered for the sake of simplicity.

For large optical distances, the internal diffuse reflectances at each interface were found in agreement with the expectation of the Lambertian approximation when absorption is negligible. In presence of absorption however, these internal reflectances slightly differ, the top one being a bit higher, and the bottom one a bit lower than the Lambertian value.

For intermediate and low optical distances (translucent material), it turns out that both internal reflectances tends to be approximately equal, and much higher than expected, which probably strongly impacts the accuracy of parameters extracted when the Lambertian value is assumed.

These results are the consequence of the competition between Fresnel reflection, which induces anisotropy in the angular distribution of radiance (low incidence angle rays may escape from the slab while high incidence angle rays remain trapped by total internal reflection), and scattering, which tends to randomize the light direction.

This work not only enables to better understand the impact of scattering within a translucent layer but also invites to revisit the well-known Saunderson correction used in 2 or 4-flux models.

Acknowledgments

This work has been funded by LABEX PRIMES (ANR-11-LABX-0063) of Université de Lyon, within the program "Investissements d'Avenir" (ANR-11-IDEX-0007) operated by the French National Research Agency (ANR) and carried out within the framework of France Life Imaging (ANR-11-INBS-0006), and also supported by a public grant from the French National Research Agency (ANR) under the Investments for the Future Program (PIA), which has the reference EUR MANUTECH SLEIGHT - ANR-17-EURE-0026.

References

[1] Schabbach L.M., dos Santos B.C., De Bortoli L.S., Fredel M.C., Henriques B., « Application of Kubelka-Munk model on the optical characterization of translucent dental zirconia », *Mater Chem Phys 2021*;258.

[2] Pop-Ciutrila IS, Ghinea R, Perez Gomez MDM, Colosi HA, Dudea D, Badea M., « Dentine scattering, absorption, transmittance and light reflectivity in human incisors, canines and molars », *J Dent 2015*;43:1116–24. doi.org/10.1016/j.jdent.2015.06.011.

[3] Kubelka P., Munk F., *Ein Beitrag zur Optik der Farbanstriche.* Z. Techn. Physik. 12, 593–601 (1931).

[4] Maheu B., Letoulouzan J.N., Gouesbet G., « Four-flux models to solve the scattering transfer equation in terms of Lorenz-Mie parameters », *Appl Opt 1984;23;3353*. https://doi.org/10.1364/ao.23.003353.

[5] Saunderson J. L., (1942) « Calculation of the color pigmented plastics », *J. Opt. Soc. Am. A 32, 727–736.*

[6] Hébert M., Hersch R.D., Emmel P., « Fundamentals of Optics and Radiometry for Color Reproduction », *Handbook of Digital Imaging*, Ed. Mickael Kriss, Wiley, New York, 1021−1077 (2015).

[7] Duveiller V., Gevaux L., Clerc R., Salomon J.-P., & Hébert M., « Reflectance and transmittance of flowable dental resin composite predicted by the two-flux model: on the importance of analyzing the effective measurement geometry », (2020, November 04).

[8] Chandrasekhar, S. (1960) *Radiative Transfer*, Dover, New York.

[9] Ishimaru, A. (1978). *Wave propagation and scattering in random media* (Vol. 2, pp. 336-393), Academic press, New York.

[10] Rogers G. L., « Optical Dot Gain in a Halftone Print », *J. Imaging Sci. Technol.*, vol. 41, nº 6, p. 643-656, (nov. 1997).

[11] Q. Fang and D. Boas, « Monte Carlo Simulation of Photon Migration in 3D Turbid Media Accelerated by Graphics Processing Units », *Opt. Express 17,* 20178-20190 (2009).

Author Biography

Arthur Gautheron graduated in 2019 from the Institut d'Optique Graduate School, France, and is now a PhD student at the University of Lyon, in the CREATIS laboratory with funding from Labex PRIMES. His research focuses on the improvement of intraoperative quantitative optical imaging for glioma resection by 5-ALA-induced PpIX fluorescence.